3-D Numerical Simulation of Water-Entry Problem by CIP based Cartesian Grid Method

Changhong Hu[1], Odd Faltinsen[2] and Masashi Kashiwagi[1]

[1] *RIAM, Kyushu University* (*hu@riam.kyushu-u.ac.jp*)

[2] *Department of Marine Technology, NTNU*

Introduction

In this paper we study the dynamics of three-dimensional body-fluid impacts by means of CFD simulation. The initial stage of impact of a ship on a free surface, i.e. slamming, has been studied extensively by analytical methods and numerical methods based on BEM assuming potential theory and neglecting gravity and air flow (e.g., Faltinsen and Zhao, 1997). However, problems that can be treated by analytical methods are restricted to two-dimensional or symmetrical three-dimensional cases with simple body geometries. A BEM is more general and flow separation from sharp corners can be handled, but it is troublesome to handle flow separation from continuously curved surfaces, e.g., spheres. On the other hand, recent development of Navier-Stokes equation based CFD methods makes it possible to treat three-dimensional complicated engineering problems. As CFD methods usually solve flows in a discrete way both in time and in space, it may be difficult to calculate impact loads accurately due to very sharply variation of pressure both temporally and spatially. Therefore the authors consider that to develop a combined analytical and CFD method, which is the goal of the current research, should be a possible approach to a practical engineering impact problem. In this stage of research, we develop a three-dimensional CFD method for this purpose. The method that is being developed and improved is a CIP (Constrained Interpolation Profile, Yabe et al. 2001) based Cartesian Grid Method.

The CIP based method proposed in this paper was developed by the authors for strongly nonlinear marine hydrodynamic problems such as slamming, water on deck, wave impact by green water, and capsizing due to large-amplitude waves (Hu and Kashiwagi, 2004). The reason for applying CIP method is from its two key features: (1) a compact support high order upwind scheme with sub-cell resolution for advection calculations and (2) a fractional step method for hydrodynamic problems in which the pressure is solved by a Poisson equation. The feature (1) helps us to obtain good accuracy for advection calculations at free surfaces and body boundaries where flow quantities vary very sharply. Owing to this feature we developed a CIP/function-transformation method as an interface capturing method for the 3-D water entry problems. The feature (2) provides us a robust flow solver for multi-phase computations, in which both compressible and incompressible flows can be treated simultaneously. In this paper we assume incompressible flows since the compressibility of the fluid is a less important factor to the studied problems. The use of incompressible flow assumption also makes the solver more computationally efficient.

A stationary non-uniform Cartesian grid is used in our method for that such grid can greatly simplify the structure of the code and increase the computation efficiency for problems with complicated free surfaces and moving bodies. Moreover, many advantages of CIP method are related to Cartesian grid. Nevertheless, the use of Cartesian grid usually has the disadvantage of its low order accuracy near body boundaries because the grids generally do not conform to the body boundaries. Efforts to improve the accuracy near the body surface have resulted in various kinds of numerical methods for Cartesian grid approach. The most famous method may be the immersed boundary method originated from the work by Peskin (1972), in which a force term is introduced to the momentum equation to describe the boundaries. Our method to handle the immersed moving boundary is designed using similar idea to the immersed boundary method.

In this extended abstract, we will briefly describe our method. Then two 3-D numerical examples, water entry of a sphere and a cylindrical body falling into a free surface will be given. The first example is compared to experimental and BEM results and reasonable good results are obtained. From the second example we show that the proposed method is robust enough to handle extremely complicated free surface development in water entry problems, such as impact with a body, breaking, merging and splash.

Governing Equations

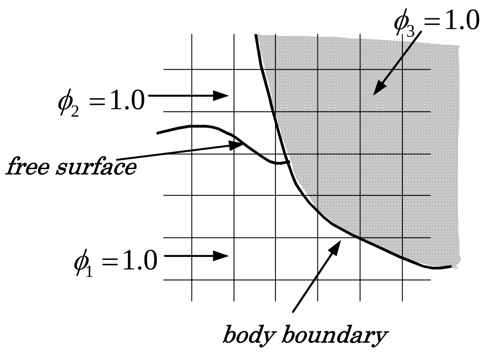

Fig.1 Density functions for multi-phase problems.

The governing equations for fluid are unsteady, viscous, incompressible Navier-Stokes equations.

$$\partial u_i / \partial x_i = 0 \tag{1}$$

$$\frac{\partial u_i}{\partial t} + u_j \frac{\partial u_i}{\partial x_j} = -\frac{1}{\rho}\frac{\partial p}{\partial x_i} + \frac{1}{\rho}\frac{\partial \sigma_{ij}}{\partial x_j} + f_i \tag{2}$$

Where σ_{ij} is the viscous stress tensor. The last term on the right-hand side of Eq. (2) denotes the an internal force, e.g., a gravity force, etc.. We also define a density function ϕ_m to distinguish different materials in a Cartesian grid, as shown in Fig.1. Here m=1, 2, 3 denote liquid, gas, and solid phases, respectively. The density function for each computational cell has the relation $\sum \phi_m = 1.0$. It can be solved by the following equation:

$$\frac{\partial \phi_m}{\partial t} + u_i \frac{\partial \phi_m}{\partial x_i} = 0 \tag{3}$$

In order to apply CIP scheme, Eqs. (2) and (3) are differentiated with respect to the spatial coordinates. Defining $\partial_\xi \chi = \partial \chi / \partial \xi \ (\xi = x_1, x_2, x_3)$, we obtain:

$$\frac{\partial(\partial_\xi \chi)}{\partial t} + u_j \frac{\partial}{\partial x_j}(\partial_\xi \chi) = -(\partial_\xi u_j)\frac{\partial \chi}{\partial x_j} + \frac{\partial H}{\partial \xi} \tag{4}$$

where χ represents each of u_i and ϕ_m in Eqs. (2) and (3), respectively. H denotes the right hand term of the equations . Equations (1-3) are the governing equations, and solved numerically by a fractional step method in which these equations are divided into an advection step and two non-advection steps.

The advection phase calculation is performed by CIP method, which is described as follows.

CIP Formulation in Three Dimensions

By CIP scheme, the profile inside a computation cell is approximated by an interpolation function. For three-dimensional case, let us consider a grid point (i, j, k), we can find an upwind cell with eight grid points: (i, j, k), (iw, j, k), (i, jw, k), (i, j, kw), (iw, jw, k), (iw, j, kw), (i, jw, kw) and (iw, jw, kw). Here, iw=i-$sign$(u_1), jw=j-$sign$(u_2) and kw=k-$sign$(u_3). The cubic polynomial we are using to approximate the spatial distribution of the value χ in the upwind cell is as follows.

$$\begin{aligned} \mathrm{X}^n(\eta_1,\eta_2,\eta_3) = \ & C_{300}\eta_1^3 + C_{030}\eta_2^3 + C_{003}\eta_3^3 + C_{111}\eta_1\eta_2\eta_3 \\ & + C_{210}\eta_1^2\eta_2 + C_{021}\eta_2^2\eta_3 + C_{102}\eta_3^2\eta_1 + C_{120}\eta_1\eta_2^2 + C_{012}\eta_2\eta_3^2 + C_{201}\eta_3\eta_1^2 \\ & + C_{200}\eta_1^2 + C_{020}\eta_2^2 + C_{002}\eta_3^2 + C_{110}\eta_1\eta_2 + C_{011}\eta_2\eta_3 + C_{101}\eta_1\eta_3 \\ & + C_{100}\eta_1 + C_{010}\eta_2 + C_{001}\eta_3 + C_{000} \end{aligned} \tag{4}$$

where $\eta_1 = x_1 - x_{1i}$, $\eta_2 = x_2 - x_{2j}$ and $\eta_3 = x_3 - x_{3k}$. Eq. (15) contains 20 unknown coefficients, C_{lmn} , which can be determined by using the known values of χ^n and $(\partial_\xi \chi)^n$ at the grid points (i, j, k), (iw, j, k), (i, jw, k) and (i, j, kw), and the value of χ^n at the grid points (iw, jw, k), (iw, j, kw), (i, jw, kw) and (iw, jw, kw). Here the superscript 'n' denotes the current time level.

Once the interpolation function is determined, the advection phase calculation is carried out by a semi-Lagrangian procedure as

$$\chi^*(\mathbf{x}) = \mathrm{X}^n(\mathbf{x} - \mathbf{u}^n \Delta t) \qquad (\partial_\xi \chi)^*(\mathbf{x}) = \frac{\partial \mathrm{X}^n}{\partial \xi}(\mathbf{x} - \mathbf{u}^n \Delta t) \tag{5}$$

where the superscript '*' denotes the time level after the advection step.

Treatment of Free Surface and Body Boundary

There are two kinds of the interface with the problem: the gas-liquid interface (free surface) and the solid-fluid interface (body boundary). Different capturing methods are developed for them.

The free surface can be captured by solving Eq. (3) about the density function of liquid ϕ_1 with CIP method. By using a function transformation $\Phi = \Phi(\phi_1)$ the sharpness of the interface can be enhanced, i.e., instead of Eq. (3) we solve the following equation with CIP method.

$$\frac{\partial \Phi}{\partial t} + u_i \frac{\partial \Phi}{\partial x_i} = 0 \tag{6}$$

Yabe et al (2001) has introduced a tangential function. Here we use a much simpler function transformation as follows:

$$\Phi(\phi_1) = 0.5 + \alpha(\phi_1 - 0.5) \quad , \quad \phi_1 = 0.5 + (\Phi - 0.5)/\alpha \tag{7}$$

where $\alpha > 1$ is the sharpness enhancement parameter. For the numerical examples shown in this paper, $\alpha = 1.2$ is sufficient to let the thickness of interface ($\phi_1 = 0.05 \to 0.95$) within 5 grid widths.

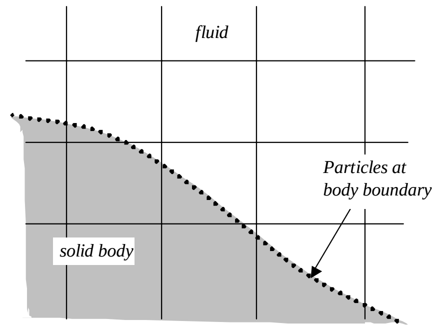

Fig. 2 Particles used to define body boundary.

For the solid body boundary, we only consider the rigid body case and we can use a Lagrangian method to directly calculate the density function for the solid phase ϕ_3 and the local velocity of the body $\hat{U}_i^{n+1}$. To numerically realize this for three-dimensional case, we use particles to approximate the body. As shown in Fig. 2, the particles are distributed on the body surface. After the hydrodynamic forces on the body are obtained, it is not difficult to calculate translational and rotational velocities at the gravity center of the rigid body, and the velocity for new time step at any particle can therefore be obtained. Then the velocity at a body boundary cell $\hat{U}_i^{n+1}$, which is required to specify as the boundary condition, can be calculated by using the velocities at the particles. Both slip and no-slip conditions for velocities at the boundary can be achieved by this method. In the present numerical solution procedure, the method of imposing the velocity distribution inside and on the body boundary is equivalent to apply a forcing term to the momentum equation. The following updating is done after the computation of Eq. (2).

$$U_i^{n+1} = \phi_3 \hat{U}_i^{n+1} + (1 - \phi_3) u_i^{**} \tag{8}$$

In boundary cell Eq. (8) is a volume fraction weighting treatment for velocity interpolation.

Numerical Results

The first computation example is the impact of a sphere with constant downward speed V on a free surface. The same problem was studied by Faltinsen and Zhao (1997) with a boundary element method. Fig. 3 and Fig. 4 show the results for the slamming coefficient $C_s = F_3/0.5\rho V^2 \pi R^2$ and the wetting factor $C_w = \eta_b/Vt$, where η_b is the free surface elevation at the body surface measured from the sphere bottom. We note that the slamming coefficient C_s is generally lower than the experimental results when $0 \le Vt/R \le 0.2$. Since the slamming force is proportional to the wetted surface and its rate of change with time, the lower predicted C_s is consistent with the lower predicted C_w.

The second example is a cylindrical body falling into a free surface as shown in Fig.5 and Fig.6. Problems like this example are expected to be studied by the proposed CFD method.

References

[1] Faltinsen, O.M. and Zhao, R., Water entry of ship sections and axisymmetric bodies, Proc. AGARD FDP workshop, Kiev, Ukraine,(1997),24.

[2] Hu, C.-H & Kashiwagi, M. A CIP method for numerical simulation of violent free surface flows. J. Mar Sci Tecnol. 9 (2004), pp. 143-157.

[3] Peskin, C.S., Flow patterns around heart valves, J. Comput. Phys. 10 (1972), 252-271,

[4] Yabe T, Xiao F and Utsumi T (2001) The Constrained Interpolation Profile Method for Multiphase Analysis. J Comput Phys 169:556-593

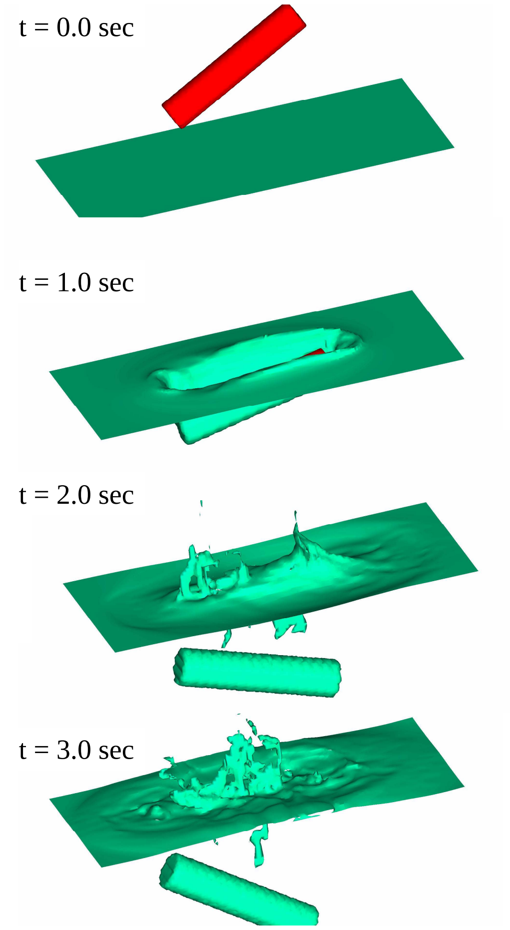

Fig.5 A cylindrical body (L=5m, D=1m) with same density as water, falling into a free surface. Initial condition is X_{G0}=0m, Z_{G0}=3m and $\alpha_2 = -\pi/6$.

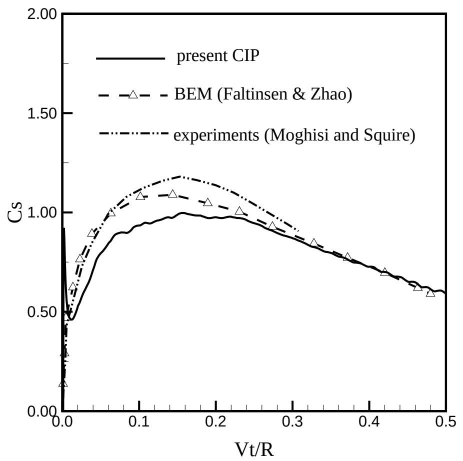

Fig. 3 Comparison of slamming coefficient

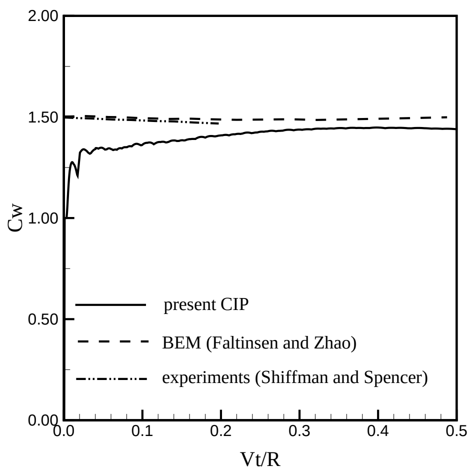

Fig.4 Comparison of wetting factor

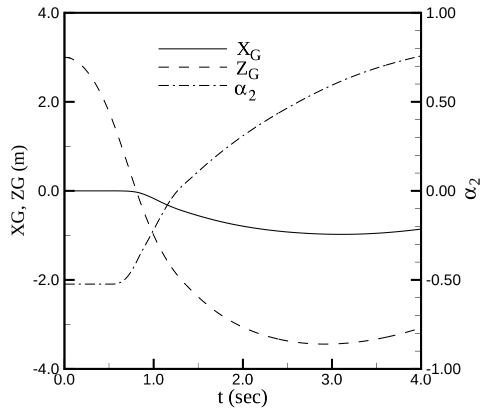

Fig.6 Time variation of gravity center positions (X_G, Z_G) and rotation angle α_2